JOURNAL OF AERONAUTICS AND SPACE TECHNOLOGIES
JULY 2010 VOLUME 4 NUMBER 4 (65-74)

ERROR ESTIMATION OF ORTHORECTIFICATION OF SMALL SATELLITE IMAGES BY DIFFERENTIAL SENSITIVITY ANALYSIS

Önder Halis BETTEMİR

Yüzüncü Yıl Üniv. İnş. Müh. Böl.
ohbettemir@yyu.edu.tr

Received: *01 NOVEMBER 2009,* ***Accepted:*** *20 JULY 2010*

ABSTRACT
By using differential sensitivity analysis, horizontal and vertical accuracy of orthorectification of monoscopic images taken by small satellites without using Ground Control Points (GCP) is predicted. The analysis is performed by differentiating the colinearity equation of orthorectification procedure with respect to the satellite's interior and exterior parameters, elevation obtained from digital elevation model (DEM) and satellite velocity. In addition to this, error of registered imaging time is estimated and the contribution of this error is also taken into account. Square of the differential equations with respect to parameters are multiplied by the variance covariance matrix of the parameters and horizontal uncertainty of the orthorectification is obtained by summing the results of this multiplication. Vertical uncertainty is caused by the uncertainty of DEM and the uncertainty of the horizontal position. Vertical uncertainty caused by the horizontal uncertainty is predicted by estimating a trend by generating a surface polynomial from DEM on the basis of covariance function of Hirvonen. Contribution of each error source is illustrated and the most sensitive parameter is obtained. Analysis results revealed that camera attitude and the image acquisition time are the most important parameters and special weight should be given in order to minimize the uncertainty of the orthorectification in the most efficient way.

Keywords: *Photogrammetry, Orthorecification, Error Propagation Law, Small Satellite*

KÜÇÜK UYDU GÖRÜNTÜLERİ ORTOREKTİFİKASYONUNUN DİFERANSİYEL HASSASİYET ANALİZİ YÖNTEMİ İLE HATA TAHMİNİ

ÖZET
Bu çalışmada diferansiyel duyarlılık analizi yöntemi ile monoskopik küçük uydu görüntülerinin yer kontrol noktası (YKN) kullanılmadan yapılan ortorektifikasyon işleminin doğruluğu kestirilmiştir. Analizler ortorektifikasyon yönteminde kullanılan kolinearite denklemlerinin uydu konumuna, yönelmesine, sayısal yükseklik modelinden (SYM) elde edilen yüksekliğe ve uydu hızına göre kısmi türevlerinin hesaplanıp hata yayılma kanunu kullanılarak ortorektifikasyon hassasiyeti tahmin edilmiştir. Bu hata kaynaklarına ilaveten bu çalışmada görüntü alınma zamanının kaydedilmesinde oluşabilecek belirsizlik de göz önüne alınmıştır. Kısmi türevlerin karesi ile ele alınan parametrelerin varyasyonu çarpılarak yatay ortorektifikasyon hatası tahmin edilmiştir. Düşey koordinatların belirsizliği ise SYM'deki belirsizlik ve yatay konumun belirsizliğinden kaynaklanmaktadır. Düşey konumdaki belirsizliğinin yatay konuma etkisi Hirvonen kovaryans fonksiyonu kullanılarak hem düz hem de eğimli olmak üzere oluşturulan iki ayrı arazi modeli üzerinde incelenmiştir. Hata kaynaklarının sonuç belirsizliğine olan etkisi hesaplanmış ve en hassas hata kaynağı belirlenmiştir. Analiz sonuçlarına göre kamera yönelmesi ile görüntüleme zamanı en hassas parametreler olarak belirlenmiştir. En etkili şekilde ortorektifikasyon hassasiyetini iyileştirebilmek için bu parametrelerin üzerinde durulması gerekmektedir.

Anahtar Kelimeler: *Fotogrametri, Ortorektifikasyon, Hata Yayılma Kanunu, Küçük Uydu.*

1. INTRODUCTION

Small satellites are usually preferred by research institutes because of their low costs. Since small ions. Weight of small satellites varies between 100 to 500 kg which also decreases the launch cost. However, solar panel and batteries of the small satellites are kept within limited sizes and as a result of this, power consumption of the on board equipment usually becomes a challenging problem. In order to keep energy consumption minimum, workload of the devices are reduced by simplifying the analytical computations. Consequently; optical sensors, attitude determination system and positioning system of small satellites are expected to have higher amounts of uncertainty. For this reason, on board sensors and devices should be preferred in a way that their sensitivities are neither too high nor too low. By this way, optimum sensor assembly can be formed in terms of economy and precision. This study aims to provide error ranges for georeferencing of images acquired by small satellites by considering several sensor assembles with typical low earth orbit and imaging geometry.

Uncertainty of automated orthorectification gives an idea about the accuracy of the orthorectified image. Uncertainty is caused by the model inputs; interior and exterior camera parameters, DEM and the uncertainty in the imaging time. These parameters have certain amount of uncertainty. This uncertainty will propagate during the automated orthorectification procedure and the final product will be effected [1]. In this study, most sensitive parameter on the orthorectification procedure is tried to be determined and possible opportunity to improve the overall orthorectification is searched. Accuracy of the most sensitive parameter should be improved as much as possible. In the s in the recording is predicted to be in the range of 1 to 5 milliseconds [5]. In this study, uncertainty of orthorectification of a monoscopic image taken by a CCD frame camera is examined.

2. METHODOLOGY

Automated orthorectification procedure is performed by using colinearity equations. The colinearity equations are based on a pin hole camera model where the camera focus, image point and the ground point are on the same line.

Colinearity equations for the CCD frame camera of a small satellite can be written as [4]:

$$X = X_0 + \left[\frac{Z - Z_0}{1 - k_1 * r^2 - k * r^4 - 2 * p_1 * x' - 2 * p_2 * y' - \frac{p_1 * r^2}{x'}} * \left[\frac{cR_{11}(x' - \Delta x) + cR_{12}(y' - \Delta y) - R_{13}f}{cR_{31}(x' - \Delta x) + R_{32}c(y' - \Delta y) + R_{33}f} \right] \right] \quad (1)$$

satellites are produced with a limited budget, most of the sensors and systems on board are chosen mainly by economical considerat

previous study, only horizontal uncertainty of automated orthorectification is predicted by differential sensitivity analysis [2]. Same method is followed in the following research, but in addition to horizontal uncertainty, vertical uncertainty is also estimated [3]. Surface run-off computations and military simulations can be given as examples which demand for accurate elevation data assigned in orthorectified images. Accuracy of vertical coordinates in automated orthorectification procedure is not only affected by accuracy of DEM, but also the uncertainty of horizontal position. This is because; during automated orthorectification procedure final vertical and horizontal ground coordinates are simultaneously computed [4]. As a result both horizontal and vertical uncertainties are mutually affected.

In this study, besides the uncertainty of interior and exterior camera parameters and DEM, error of the recording of the image acquisition time is also taken into account. In most of the small satellites the satellite clock error is synchronized with the clock of the on board GPS receiver. For this reason, clock bias of the satellite clock is small enough to be neglected. However, the CPU installed on the satellite may perform multi-task operations which are handled according to the pre-assigned priority rules. If the satellite CPU is busy during the image acquisition, the acquisition time may not be recorded correctly by the CPU of the satellite. There might be random delays in the recording of the image acquisition time. The amount of delay

$$Y = Y_0 + \left[\frac{Z - Z_0}{1 - k_1 * r^2 - k_2 * r^4 - 2 * p_2 * y' - 2 * p_1 * x' - \frac{p_2 * r^2}{y'}} * \left[\frac{cR_{21}(x' - \Delta x) + cR_{22}(y' - \Delta y) - R_{23}f}{cR_{31}(x' - \Delta x) + R_{32}c(y' - \Delta y) + R_{33}f} \right] \right] \quad (2)$$

where

$$R = \begin{bmatrix} \cos\phi\cos\kappa & -\cos\phi\sin\kappa & \sin\phi \\ \sin\omega\sin\phi\cos\kappa + \cos\omega\sin\kappa & -\sin\omega\sin\phi\sin\kappa + \cos\omega\cos\kappa & -\sin\omega\cos\phi \\ -\cos\omega\sin\phi\cos\kappa + \sin\omega\sin\kappa & \cos\omega\sin\phi\sin\kappa + \sin\omega\cos\kappa & \cos\omega\cos\phi \end{bmatrix}$$

r is the distance of the corresponding pixel from the principal point on the CCD array (mm) ; x', y' values are the image coordinates; k_1 and k_2 are radial lens distortion parameters; p_1 and p_2 are decentering lens distortion parameters; f is the focal length of the camera; c is the size of the sensing element on the CCD frame; Δx Δy are the principal coordinates; X_0, Y_0 and Z_0 are the Cartesian camera coordinates; Z is the elevation of the ground point; X and Y are the horizontal coordinates of the ground point. ω, φ and κ are the attitude angles between the body fixed reference system S_B and orbital reference system S_O. The rotation matrix from S_B to S_O is obtained by

rotating the Y axis by φ, X axis by ω and finally the Z axis by κ angle respectively. At the end of the Euler rotations following the rotation order; φ, ω and κ the matrix R is obtained.
After obtaining the initial ground positions of the image coordinates, with the help of DEM, relief displacement of the initial ground position is computed and the initial ground position is corrected. Initially since the elevation of the ground point is not known (1) and (2) are solved by assuming the elevation of the ground point is zero. After computing the initial ground coordinates, elevation of the initial ground point is obtained from DEM and then the (1) and (2) are solved again with the updated elevation. The iteration is continued until the differences between the two elevation values are small enough.

The Universal Transverse Mercator (UTM) projection system is preferred for georeferencing. BilSAT orbit and attitude values at the date of 3rd of August 2005 at time 7:27:46 are used in this analysis. The imaged area is the region of Ankara, Turkey.

Camera position and the attitude are obtained from the telemetry of the satellite. Because of the imperfections of the sensors there will be an uncertainty in the position and attitude of the camera. Uncertainty in DEM also contributes to the total uncertainty of the computed ground coordinates. In addition to this, time keeping error of image acquisition contributes to the total uncertainty. Uncertainty of the computed ground coordinates is predicted by the differential analysis.

Differential analysis is based on Taylor series expansion to approximate the response of the model to changes in the model's parameters under consideration. Base values, ranges and distributions are selected for the input variables. The model including the input variables and the output is written as [6]:

$$\boldsymbol{y} = f(x) \tag{3}$$

where,

$$\boldsymbol{y} = f(X_0, Y_0, Z_0, \omega, \phi, \kappa, \Delta x, \Delta y, k_1, k_2, p_1, p_2, h, \delta t)$$

Base value represents the most probable value that the parameter can be assigned. Base values of the interior camera parameters are calculated after the camera calibration procedure and exterior camera parameters are obtained from the telemetry. Finally base value of elevation is provided from DEM. In this study SRTM DEM is used, which is produced by the Shuttle Radar Topography Mission (SRTM). Accuracy of SRTM DEM is estimated to be within a range of 5 meters [7]. Uncertainty ranges of the variables are obtained by the accuracy declarations of the manufacturers [8 – 12]. Ranges of the interior parameters are obtained from the variance covariance matrix of the parameter estimation. In addition to this, the interior camera parameters can be obtained by ground tests, however due to immense vibrations during the launch of the satellite, it is expected that the initial interior camera parameters should be updated after the launch of the satellite.

Distribution of the parameters is considered as normal. Uncertainties of the satellite interior and exterior camera parameters and DEM can be considered as normally distributed which are plus or minus in equal probability while uncertainty in the recording of the image acquisition time will always positive (delay) due to the characteristics of the error source. In order to handle uncertainty of recording of the image acquisition time together with the uncertainties of the other parameters the following assumption is made.

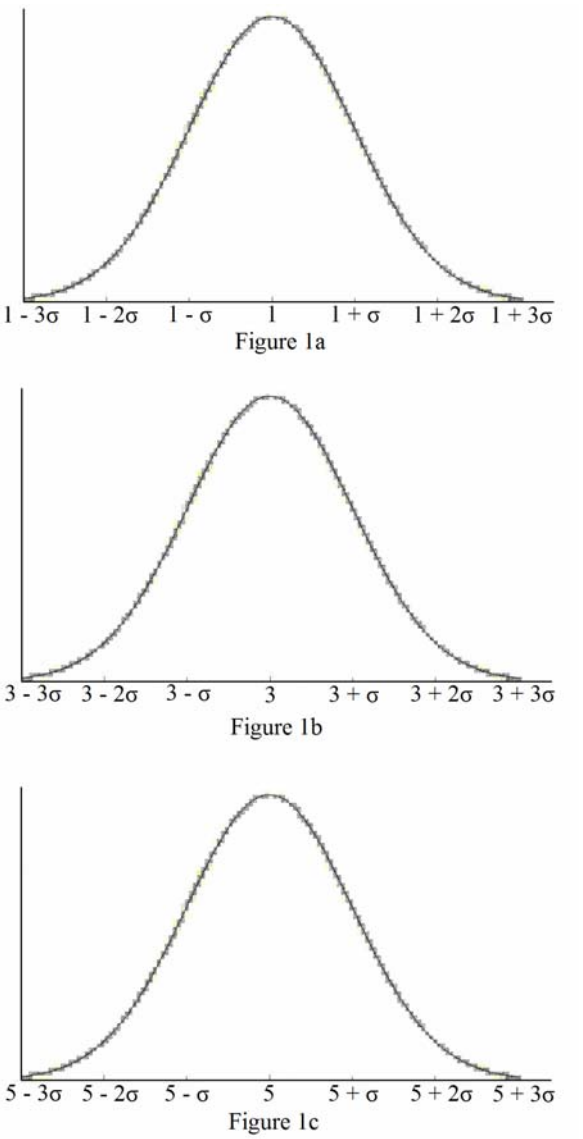

Figure 1 Uncertainty distribution of timing delay

Satellite CPU is assumed to be under three different workloads: low, medium and high. The most probable delays in the recording of image acquisition time are

assumed to be 1 millisecond, 3 milliseconds and 5 milliseconds respectively. Probability distributions of the assumed delays under certain CPU workload within three sigma range of the three cases are given in Figure 1.

Distribution of image acquisition time bias is expected to be skewed. However, in order to simplify uncertainty estimation calculations and apply error propagation law, the distributions are assumed to be normal. The assumed distributions cover almost whole events. Only 1% of the events are not covered which are not in the three-sigma range. The events outside of this range can be neglected. In order to simplify computations of uncertainty estimation, the standard deviation of the delay in recording the image acquisition time is assumed to be one third of the expected delay. With this modification on the uncertainty distribution functions, it will be possible to apply error propagation law. The three-sigma range is preferred because if the uncertainty distribution function is obtained by using four-sigma range, than the standard deviation of the uncertainty would be underestimated. If the distribution functions are obtained by using two-sigma range, then the uncertainty would be overestimated and the distribution function will cover only 68% of the events.

Workload of satellite CPU is pre-known by ground station and the most suitable workload range among the three classes can be assigned. Then necessary correction for the image acquisition time record error is performed which leads to an uncertainty in the image acquisition time. The standard deviations of the uncertainties are assumed to be $\pm 1/3$ ms, ± 1 ms and $\pm 5/3$ ms for the low, medium and high CPU workloads respectively.

Evaluation of the partial derivatives is the most demanding part of the differential analysis. For this reason, second order Taylor series expansion is avoided in this study. First order Taylor series approximation is used for the approximation of the effect of input parameters on the output variables. First order Taylor Series expansion approximating function y can be written as [6]:

$$y(\boldsymbol{x}) = y(\boldsymbol{x}_o) + \sum_{i=1}^{n} \left[\frac{\partial f(\boldsymbol{x}_o)}{\partial x_i} \right] (x_i - x_{io}) \tag{4}$$

where, $\boldsymbol{x}_o$ is the vector of input parameters with the corresponding base values and x_i is the value of the i^{th} input parameter within its range.

Variance propagation technique is used to estimate the uncertainty in y. Error propagation law with first order Taylor series ends up with the following equations[4]:

$$E(y) = y(\boldsymbol{x}_o) + \sum_{i=1}^{n} \left[\frac{\partial f(\boldsymbol{x}_o)}{\partial x_i} \right] E(x_i - x_{io}) \tag{5}$$

$$E(y) = y(\boldsymbol{x}_o) \tag{6}$$

where, E denotes the expected value. Variance is computed by the following formula [6]:

$$V(y) = y(\boldsymbol{x}_o) + \sum_{i=1}^{n} \left[\frac{\partial f(\boldsymbol{x}_o)}{\partial x_i} \right]^2 V(x_j) + 2 \sum_{i=1}^{n} \sum_{j=i+k}^{n} \left[\frac{\partial f(\boldsymbol{x}_o)}{\partial x_i} \right] \left[\frac{\partial f(\boldsymbol{x}_o)}{\partial x_j} \right] Cov(x_i, x_j) \tag{7}$$

where, V is variance of the output variable and Cov is variance covariance matrix of the parameters

Since first order Taylor series expansion is used for the estimation of y, the contribution of parameters to the variance of y can be estimated with the ratio shown below [6]:

$$\sum_{i=1}^{n} \left[\frac{\partial f(\boldsymbol{x}_o)}{\partial x_i} \right]^2 \frac{V(x_j)}{V(\boldsymbol{y})} \tag{8}$$

Fractional contributions to variance can be used to order the parameters with respect to their contribution to the uncertainty in y. This ordering is based on both the absolute effect of the parameter, as measured with their partial derivatives, and the effect of distributions assigned to the parameter, as measured by $V(x_i)$.

After estimating the uncertainty of horizontal positioning, uncertainty of the vertical coordinate can be estimated. The actual direction from CCD frame camera differs from the computed direction by using the on-board sensors. The solid line in Figure 2 represents the true direction of light array and the dashed line represents the estimated direction. As this is the case, the elevation data retrieved from DEM will be h_1, although h_0 should be retrieved. The difference between h_0 and h_1 is estimated by assuming two different topographic surfaces. Minimum deviation and maximum deviation bounds are estimated from the smooth and steep surfaces. The smooth and steep surfaces are formed by extracting 10x10 elevation points which covers approximately 900m x 750m region. Ground point of interest is assumed to be at the center of the region which is modeled by surface polynomials.

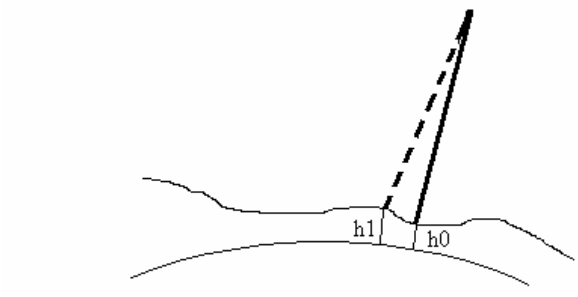

Figure 2 Effect of horizontal uncertainty

When generating the surface higher weight is assigned to the nearer points. Weights are assigned by using the covariance function of Hirvonen [13, 14]:

$$\sigma_{i,j}^2 = \frac{1}{1+\left(\frac{l}{c}\right)^2} \tag{9}$$

where, l is the horizontal distance between points i and j and c is the correlation length which amounts to 12.2 meters. Coefficients of the surface polynomial are computed by Gauss Markoff model;

$$\hat{\beta} = (X'WX)^{-1}X'Wy \tag{10}$$

where W is the weight matrix formed by Hirvonen covariance function. β is the parameters of the surface polynomial given in Equation (11).

$$h = a_0 + a_1 N + a_2 E + a_3 N^2 + a_4 E^2 + a_5 NE \tag{11}$$

Uncertainty of elevation caused by horizontal uncertainty is estimated by the error propagation law which is given in Equation (12).

$$\sigma_{hu}^2 = \sqrt{\left(\frac{\partial h}{\partial E}\sigma_E\right)^2 + \left(\frac{\partial h}{\partial N}\sigma_N\right)^2} \tag{12}$$

where E is the Easting and N is the Northing and σ_E and σ_N are the uncertainties in the computed east and North coordinates. Total uncertainty of vertical coordinates is obtained by adding the uncertainty of DEM and uncertainty caused by horizontal uncertainty.

$$\sigma_h^2 = \sigma_{hu}^2 + \sigma_{DEM}^2 \tag{13}$$

3. IMPLEMENTATION

For the implementation of the system, typical camera technical specifications suitable for small satellites are assumed for the camera model. Since the analysis is based on the simulated data, lens distortion parameters and the principal coordinate values are assumed. For these parameters, typical optical parameters for a small satellite are assigned which is given in Table 1. Focal length f and size of the sensing elements of the CCD array c are assigned which ends up with typical values for the small satellites. The orbit of the satellite is assumed to be around 680 kms from the ground which corresponds to around 10 meters of spatial resolution. Δx and Δy are the x and y coordinates of the principal point. These two parameters models the imperfection in the production of the camera in which the center of the CCD Frame sensor can not be exactly placed through the boresight. The lens distortion is modeled by four parameters; k_1, k_2, p_1 and p_2.

Table 1 Assumed values for interior camera parameters

Parameter	Value
f	500 mm
c	0.0074 mm/pixel
Δx	0.01mm
Δy	0.01mm
k_1	0.00001 1/mm2
k_2	1,00E-16 1/mm4
p_1	1,00E-10 1/mm
p_2	1,00E-10 1/mm

Accuracy of the GPS receiver and star camera are obtained from the declarations of manufacturers. For the sensitivity and uncertainty analysis of the orthorectification, six different star trackers and 2 different GPS positioning techniques are examined. Only one DEM, SRTM DEM and three different on-board CPU workloads are examined. The uncertainty values for the star tracker, GPS positioning, DEM and image acquisition time recording are given in table 2 [7 – 11].

Table 2 Uncertainty values for exterior parameters, elevation and image acquisition record time

STC	GPS	DEM	δt
150 asec	10 m	5 m	1/3 ms
30 asec	1 m		1 ms
15 asec			5/3 ms
6 asec			
3 asec			
1 asec			

Uncertainty computation procedure mentioned in (7) can be written in matrix form as in Equation (14) and (15):

$$\sigma_X^2 = \boldsymbol{X}_X \boldsymbol{D} \boldsymbol{X}_X^T \tag{14}$$

$$\sigma_Y^2 = \boldsymbol{X}_Y \boldsymbol{D} \boldsymbol{X}_Y^T \tag{15}$$

where

$$\boldsymbol{D} = \begin{bmatrix} \sigma_f^2 & & & & & & & & & & & & & & \\ & \ddots & & & & & & & & & & & & & \\ & & \sigma_\omega^2 & \sigma_\omega\sigma_\phi & \sigma_\omega\sigma_\kappa & & & & & & & & & & \\ & & \sigma_\phi\sigma_\omega & \sigma_\phi^2 & \sigma_\phi\sigma_\kappa & & & & & & & & & & \\ & & \sigma_\kappa\sigma_\omega & \sigma_\kappa\sigma_\phi & \sigma_\kappa^2 & & & & & & & & & & \\ & & & & & \sigma_X^2 & \sigma_X\sigma_Y & \sigma_X\sigma_Z & & & & & & & \\ & & & & & \sigma_Y\sigma_X & \sigma_Y^2 & \sigma_Y\sigma_Z & & & & & & & \\ & & & & & \sigma_Z\sigma_X & \sigma_Z\sigma_Y & \sigma_Z^2 & & & & & & & \\ & & & & & & & & \ddots & & & & & & \\ & & & & & & & & & \sigma_h^2 & & & & & \end{bmatrix}$$

$$\boldsymbol{X}_X = \begin{bmatrix} \frac{\partial X}{\partial X_0} & \frac{\partial X}{\partial Y_0} & \frac{\partial X}{\partial Z_0} & \frac{\partial X}{\partial \omega} & \frac{\partial X}{\partial \phi} & \frac{\partial X}{\partial \kappa} & \frac{\partial X}{\partial \Delta x} & \frac{\partial X}{\partial \Delta y} & \frac{\partial X}{\partial k_1} & \frac{\partial X}{\partial k_2} & \frac{\partial X}{\partial p_1} & \frac{\partial X}{\partial p_2} & \frac{\partial X}{\partial h} & \frac{\partial X}{\partial \delta t} \end{bmatrix}$$

$$\boldsymbol{X}_Y = \begin{bmatrix} \frac{\partial Y}{\partial X_0} & \frac{\partial Y}{\partial Y_0} & \frac{\partial Y}{\partial Z_0} & \frac{\partial Y}{\partial \omega} & \frac{\partial Y}{\partial \phi} & \frac{\partial Y}{\partial \kappa} & \frac{\partial Y}{\partial \Delta x} & \frac{\partial Y}{\partial \Delta y} & \frac{\partial Y}{\partial k_1} & \frac{\partial Y}{\partial k_2} & \frac{\partial Y}{\partial p_1} & \frac{\partial Y}{\partial p_2} & \frac{\partial Y}{\partial h} & \frac{\partial Y}{\partial \delta t} \end{bmatrix}$$

When the pixel position changes, it is clear that the partial derivatives with respect to parameters will change. For this reason, the uncertainty analysis is repeated for 3 different image positions; (1,1), (1024,1024) and (2048, 2048).

First uncertainty analysis is performed with 150 arc second precise STC, 10 m precise GPS and 5 m precise DEM. Workload of the on-board CPU is assumed as high and the following results given in Table 3 are obtained. The analysis results consist of two parts. In the first part the uncertainty of the Northing is represented for the three image positions. The sensitivities of camera position, star tracker, DEM and image acquisition time, δt, on computed Northing are represented in the first four columns which are under the sensitivity subtitle. Horizontal uncertainty and vertical uncertainty caused by horizontal uncertainty is represented under uncertainty title. In the three columns, horizontal uncertainties, vertical uncertainty caused by horizontal uncertainty if the region is smooth and vertical uncertainty caused by horizontal uncertainty if the region is steep sloped are represented. In the second part, same analysis is repeated for Easting.

Table 3 Uncertainty values of analysis 1

Northing (m)						
Sensitivity				**Uncertainty (m)**		
POS	**ATT**	**DEM**	**Δt**	**H U**	**VU sm**	**VU st**
0,0003	0,9958	0,0000	0,0037	183,785	2,347	8,498
0,0003	0,9961	0,0000	0,0037	183,271	2,340	8,474
0,0003	0,9957	0,0000	0,0037	182,767	2,334	8,451
Easting (m)						
Sensitivity				**Uncertainty (m)**		
POS	**ATT**	**DEM**	**Δt**	**H U**	**VU sm**	**VU st**
4e-05	0,9998	1e-06	3e-05	499,023	7,016	15,006
4e-05	0,9999	1e-06	3e-05	499,049	7,016	15,007
4e-05	0,9998	1e-06	3e-05	498,904	7,014	15,003

As seen in Table 3 star camera is the most sensitive device as the attitude elements are the most sensitive. Uncertainty of northing is significantly less than the uncertainty of easting. The reason for this can be explained as the precision of the star tracker in roll angle is less than the precision of pitch and yaw angles. Within this exterior camera geometry, in other words orbit characteristics and camera attitude, positional uncertainty of northing is significantly less than the uncertainty of easting.

Uncertainty of vertical coordinates due to horizontal uncertainty can be as high as 15 meters which is extremely a high value. Total uncertainty of vertical direction can be as high as 17 meters when uncertainty of DEM and the vertical uncertainty caused by uncertainty of latitude are added. Total uncertainty of vertical coordinates is significantly higher than the uncertainty of DEM. Although this is the case, horizontal uncertainty and sensitivity values are not updated. The reason behind this is the very low sensitivity of uncertainty of elevation on the horizontal coordinates. The image is almost in nadir direction and as a result of this the unit change in vertical direction causes significantly small change in horizontal direction. In addition to this, the uncertainty of horizontal direction is too much that the contribution of second order terms can easily be neglected. Since the most sensitive parameter is camera attitude the precision of the star tracker must be improved. The analysis is repeated with a more precise star tracker which has 30 arc second precision and the obtained results are shown in Table 4.

Table 4 Uncertainty values of analysis 2

Northing (m)						
Sensitivity				**Uncertainty (m)**		
POS	**ATT**	**DEM**	**δt**	**H U**	**VU sm**	**VU st**
0,0060	0,9041	8e-05	0,0829	38,576	0,493	1,784
0,0061	0,9100	8e-05	0,0838	38,349	0,490	1,773
0,0061	0,9031	8e-05	0,0837	38,382	0,490	1,775
Easting (m)						
Sensitivity				**Uncertainty (m)**		
POS	**ATT**	**DEM**	**δt**	**H U**	**VU sm**	**VU st**
0,0009	0,9958	3e-05	0,0007	100,006	1,406	3,007
0,0009	0,9983	3e-05	0,0007	99,889	1,404	3,004
0,0009	0,9958	3e-05	0,0007	99,983	1,406	3,007

Sensitivity of the camera attitude is still the highest parameter, but significant improvement is achieved in the overall precision of the orthorectification. As the uncertainty of horizontal coordinates decreased, the uncertainty of vertical coordinate due to uncertainty of horizontal coordinates also decreased. When the variances of the vertical uncertainties are added, it is seen that total uncertainty of vertical coordinate is only 1 meter more than uncertainty of DEM. Although by improving the precision of star tracker the uncertainties of the vertical and horizontal coordinates decreased significantly, sensitivity of the camera attitude is close to 1 especially in easting. Since attitude of the satellite is still the most sensitive parameter, in the next analysis better star tracker

which has 15 arc second precision had been used and the obtained results are given in Table 5.

When the results of analysis 3 is examined it is seen that sensitivity of the image acquisition and camera position has been increased significantly but they are still negligible compared with the sensitivity of camera attitude, which is the most sensitive parameter still close to 1 especially in the direction of easting. When the sensitivities of the parameters in northing are examined it is seen that besides camera attitude, sensitivity of image acquisition time is also high. Sensitivity of the examined parameters are higher at the image center. The reason for this can be expressed as the lens distortion effect diminishes at the image center and reaches its maximum at the image corners. Because of this, at the image center sensitivity of the parameters other than lens distortion parameters are higher.

Table 5 Uncertainty values of analysis 3

Northing (m)						
Sensitivity				**Uncertainty (m)**		
POS	**ATT**	**DEM**	**Δt**	**H U**	**VU sm**	**VU st**
0,0188	0,7021	0,0002	0,2574	21,887	0,279	1,012
0,0193	0,7164	0,0003	0,2640	21,610	0,276	0,999
0,0189	0,6997	0,0002	0,2594	21,803	0,278	1,008
Easting (m)						
Sensitivity				**Uncertainty (m)**		
POS	**ATT**	**DEM**	**Δt**	**H U**	**VU sm**	**VU st**
0,0036	0,9834	0,0001	0,0028	50,317	0,707	1,513
0,0036	0,9934	0,0001	0,0029	50,068	0,704	1,506
0,0036	0,9834	0,0001	0,0028	50,307	0,707	1,513

Significant improvement is obtained by improving the precision of the star tracker. As the camera attitude is still the most sensitive parameter, it is necessary to install more precise star tracker which has 6-arc second accuracy. Analysis results obtained with this configuration is given in Table 6.

Table 6 Uncertainty values of analysis 4

Northing (m)						
Sensitivity				**Uncertainty (m)**		
POS	**ATT**	**DEM**	**Δt**	**H U**	**VU sm**	**VU st**
0,0458	0,2738	0,0006	0,6274	14,019	0,179	0,631
0,0484	0,2879	0,0006	0,6631	13,636	0,174	0,613
0,0459	0,2715	0,0006	0,6291	14,000	0,179	0,631
Easting (m)						
Sensitivity				**Uncertainty (m)**		
POS	**ATT**	**DEM**	**Δt**	**H U**	**VU sm**	**VU st**
0,0204	0,9046	0,0008	0,0162	20,985	0,295	0,648
0,0217	0,9603	0,0008	0,0172	20,370	0,286	0,631
0,0204	0,9043	0,0008	0,0162	20,984	0,295	0,647

Camera attitude is still the most sensitive parameter in easting, however in northing image acquisition time is the most sensitive parameter. Due to the precision characteristics of star trackers and imaging geometry, sensitivity of the camera attitude on ground coordinates is higher on easting than northing. In contrast with this, sensitivity of image acquisition time is higher on northing. With this technical specification of small satellites, it will be possible to produce automated orthorectified maps with reasonable orthorectification accuracy. 24 meters of horizontal uncertainty and 5.5 meters of vertical uncertainty of orthorectification error can be accepted as reasonable for many civil applications. On the other hand, if more precise orthophotos are needed it can be a good alternative to image when the workload of the on-board CPU is medium. Because installing a better star tracker may cost more than delaying some of the tasks which have high computational demand. The analysis results obtained when the CPU workload is medium is given in Table 7.

Table 7 Uncertainty values of analysis 5

Northing (m)						
Sensitivity				**Uncertainty (m)**		
POS	**ATT**	**DEM**	**δt**	**H U**	**V U sm**	**VU st**
0,074	0,441	0,001	0,400	11,044	0,141	0,511
0,081	0,481	0,001	0,438	10,554	0,135	0,488
0,074	0,438	0,001	0,401	11,019	0,141	0,510
Easting (m)						
Sensitivity				**Uncertainty (m)**		
POS	**ATT**	**DEM**	**δt**	**H U**	**V U sm**	**VU st**
0,021	0,914	0,001	0,006	20,876	0,293	0,628
0,022	0,971	0,001	0,006	20,258	0,285	0,609
0,021	0,914	0,001	0,006	20,874	0,293	0,628

Imaging when the on board CPU has medium workload decreased the sensitivity of error of image acquisition time recording when compared with the analysis results with high CPU workload. With this parameter configuration image acquisition time is again the second most sensitive parameter after the attitude as seen in Table 7. Uncertainty in Northing decreased significantly which represents the characteristics of the error source. Because of the BilSAT satellite's orbit characteristic, which is a retrogate orbit close to polar orbit the satellite moves almost parallel to the north direction. Uncertainty related with the imaging time will cause an uncertainty in the position of the satellite. However, this uncertainty differs from the uncertainty caused by the positioning with the on-board GPS receiver. Uncertainty in time causes an uncertainty on the direction of velocity of the satellite. For this reason, the uncertainty related with the imaging time ends up

with significantly more uncertainty in the northing. The amount of the uncertainty depends on the satellite velocity with respect to earth fixed reference frame and the uncertainty of image acquisition.

If uncertainty in ground coordinates is to be decreased, camera attitude is the most sensitive parameter. In the next analysis 3 arc second precision star tracker has been used. Analysis results are given in Table 8.

In this configuration image acquisition time is the most sensitive parameter and the sensitivity of camera position is close to sensitivity of camera attitude if uncertainty of northing is considered. However, there is still a significant difference for the uncertainty of easting, in which sensitivity of the camera attitude is the highest. In this case the uncertainties of the northing and easting are close to each other. This means that uncertainty caused by uncertainty in camera attitude parameters are close to the uncertainty caused by the uncertainty in the image acquisition time.

Table 8 Uncertainty values of analysis 6

Northing (m)						
Sensitivity				**Uncertainty (m)**		
POS	**ATT**	**DEM**	**δt**	**H U**	**V U sm**	**V U st**
0,110	0,165	0,001	0,597	9,033	0,115	0,352
0,126	0,188	0,002	0,684	8,440	0,108	0,318
0,110	0,163	0,001	0,598	9,028	0,115	0,352
Easting (m)						
Sensitivity				**Uncertainty (m)**		
POS	**ATT**	**DEM**	**δt**	**H U**	**V U sm**	**V U st**
0,066	0,727	0,002	0,019	11,705	0,165	0,418
0,081	0,893	0,003	0,023	10,561	0,148	0,390
0,066	0,726	0,002	0,019	11,709	0,165	0,417

In order to prevent increasing the cost of the satellite, the workload of the satellite is decreased to low in order to decrease the uncertainty. The analysis results with this camera configuration are given in Table 9.

Table 9 Uncertainty values of analysis 7

Northing (m)						
Sensitivity				**Uncertainty (m)**		
POS	**ATT**	**DEM**	**δt**	**H U**	**VU sm**	**V U st**
0,2381	0,3559	0,0031	0,1305	6,148	0,079	0,284
0,3281	0,4878	0,0043	0,1798	5,238	0,067	0,242
0,2387	0,3528	0,0031	0,1308	6,141	0,078	0,284
Easting (m)						
Sensitivity				**Uncertainty (m)**		
POS	**ATT**	**DEM**	**δt**	**H U**	**VU sm**	**VU st**
0,0668	0,7392	0,0025	0,0021	11,607	0,163	0,349
0,0824	0,9119	0,0031	0,0026	10,452	0,147	0,314
0,0668	0,7384	0,0025	0,0021	11,611	0,163	0,349

By decreasing the workload of the CPU to low, the image acquisition time becomes the third most sensitive parameter. Uncertainty of northing is decreased significantly which was an expected result due to characteristics of the error source.

Commercially, star trackers with a precision of 1 arc second are available. However, those star trackers are not available for small satellites because of their high costs, dimensions and power consumptions. In contrast with this, with the improvements of technology reduction in weight, cost and power demand is expected. Consequently, in the near future 1 arc second precision star trackers can be available for small satellites. In the next analysis 1 arc second precision star tracker is used and the results are given in Table 10.

In this case the sensitivity of the camera position on ground coordinates is more than the sensitivity of camera attitude in northing. Also the uncertainty of northing and easting became close to each other as the significance of the precision difference between the roll and pitch and yaw angles are reduced. At this point improving the uncertainty of the orthorectification procedure will be too expensive for the small satellites by improving the accuracy of the star tracker. In addition to this, sensitivity of the camera position is more significant. In the previous analysis it is assumed that the small satellite is equipped with a single frequency GPS receiver performing absolute positioning with 10 meter precision. The positional accuracy can be improved by installing a dual frequency GPS receiver up to 1 meter. In this case, the 1 meter precision may not be obtained real time due to the power and computational limitations of the small satellites. This is because the analysis results are obtained by assuming the workload of the CPU as low. The post processing will not prevent the automated orthorectification. In this case, the whole GPS receiver output may have to be downloaded and after processing the data with software 1 meter of precision be obtained. The analysis is repeated with 1 meter uncertainty in camera position and the analysis results are given in Table 11.

Table 10 Uncertainty values of analysis 8

Northing (m)						
Sensitivity				**Uncertainty (m)**		
POS	**ATT**	**DEM**	**δt**	**H U**	**VU sm**	**VU st**
0,348	0,058	0,005	0,191	5,083	0,065	0,204
0,579	0,096	0,008	0,317	3,942	0,050	0,137
0,348	0,057	0,005	0,191	5,088	0,065	0,205
Easting (m)						

Sensitivity				Uncertainty (m)		
POS	ATT	DEM	δt	H U	VU sm	VU st
0,195	0,240	0,007	0,006	6,797	0,096	0,235
0,435	0,535	0,016	0,014	4,549	0,064	0,182
0,194	0,239	0,007	0,006	6,807	0,096	0,235

There is not a notable improvement in the overall positional uncertainty although the uncertainty of the camera position is reduced significantly. The reason of this situation is mainly the geometry of the uncertainty of the positioning with GPS. GPS positioning results in precise horizontal coordinates but imprecise vertical coordinates. As a result horizontal position of the GPS receiver is obtained more precisely than the altitude of the satellite. Fortunately, the uncertainty of the altitude of the satellite does not contribute to the overall uncertainty of the ground coordinates as much as the horizontal coordinates. Consequently, the 1 meter uncertainty of the camera position does not significantly contribute to the overall positioning uncertainty. This can be easily inferred from the low sensitivity values of the camera position.

Table 11 Uncertainty values of analysis 9

Northing (m)						
Sensitivity				Uncertainty (m)		
POS	ATT	DEM	δt	H U	VU sm	VU st
0,005	0,088	0,007	0,291	4,115	0,053	0,184
0,014	0,224	0,018	0,744	2,574	0,033	0,103
0,005	0,087	0,007	0,291	4,120	0,053	0,184
Easting (m)						
Sensitivity				Uncertainty (m)		
POS	ATT	DEM	δt	H U	VU sm	VU st
0,002	0,297	0,009	0,008	6,106	0,086	0,190
0,008	0,939	0,029	0,024	3,433	0,048	0,119
0,002	0,296	0,009	0,008	6,118	0,086	0,190

At the center of the image, the uncertainty of the camera attitude is extremely high. The reason of this is the disappearing of the lens distortion effects at the image center. If camera attitude had been determined precisely, sensitivity of the error sources would change significantly in different positions on the image. However overall uncertainty in the horizontal coordinates are small enough for an automated orthorectification and the produced image-map can safely be used in any application. In addition to this, uncertainty of DEM and uncertainty of vertical coordinates caused by horizontal uncertainty does not contribute significantly to the overall uncertainty of the orthorectification. The reason of this can be explained by imaging geometry. Roll, pitch and yaw angles of the satellite are measured as 7.5643, -1.4771 and 0.4629 degrees respectively at the imaging moment. As a result the maximum zenith angle is less than 11 degrees which is computed at the upper left corner of the image. The image is taken almost through nadir direction and the effect of the relief is very low. As a result for the horizontal position of the orthorectification there is not any requirement for a high precision DEM.

4. CONCLUSION

In this study, the effect of uncertainty of interior and exterior camera parameters, DEM and image acquisition time on the orthorectification uncertainty is examined. Camera attitude has significant effect on the overall orthorectification uncertainty. Image acquisition time has moderate effect on northing. In addition to this, it is seen that the uncertainty of the camera position does not contribute to the overall orthorectification uncertainty considerably.

Uncertainty of the horizontal position increases the uncertainty of the DEM since the elevation obtained from the DEM will not be the true elevation of that specific region. However, increment in the uncertainty of DEM due to uncertainty in the horizontal position depends on the geographical conditions of the region. If there are steep slopes in the region, increase in the uncertainty of the assigned elevation would be unavoidably large.

Because of the imaging geometry of the CCD frame cameras, the uncertainties of camera attitude and image acquisition time are not expected to end up with distortion in the image. In other words, the north direction may be wrong in the image but the amount of misalignment would be constant in whole portions of the image. In addition to this, large artificial objects such as airports can in a rotated state but they would not be distorted. Namely, the shapes would be preserved and the horizontal uncertainty will not distort the image.

In the analyses it is seen that if the horizontal uncertainty is not too high, uncertainty of vertical coordinates are not affected significantly and uncertainty of DEM is the main error source of the vertical uncertainty. This inference can easily be seen if the first two analyses are examined. Effect of horizontal uncertainty on vertical uncertainty diminishes rapidly in the succeeding analyses.

Image acquisition time and camera attitude are the most important parameters. Because of the exterior imaging geometry and satellite orbit they affect different outputs. Camera attitude mainly effects easting and image acquisition time mainly effects northing. If the contributions of these two uncertainties are kept close to each other as much as possible it will be possible to produce precise orthorectified images with a reasonable hardware cost.

5.ACKNOWLEDGMENT

The author would like to thank Tübitak Uzay for the orbit data and camera characteristic of mini satellite BilSAT.

6.REFERENCES

[1] Karl Rudolf Koch "Parameter Estimation and Hypothesis Testing in Linear Models", Second Edition Springer 1999.

[2] Bettemir Ö. H., "Differential Sensitivity Analysis for the Accuracy Estimation of Orthorectification of Small Satellite Images", Proceedings of the International Workshop on Small Satellites, New Missions and New Technologies SSW 2008, June 05 – 07, 2008, İstanbul Turkey.

[3] Bettemir Ö. H., "Differential Sensitivity Analysis for the Orthorectification of Small Satellite Images", Proceedings of the 4th International Conference on Recent Advances on Space Technologies, RAST 2009, June 11 – 13, 2009, İstanbul Turkey.

[4] Karl Krauss, "Photogrammetry Volume 1 Fundamentals and Standard Processes" Dümmler 1993 Bonn

[5] http://www.uzay.tubitak.gov.tr/ visited on: 16.07.2010

[6] J. C. Helton, "Uncertainty and Sensitivity Analysis Techniques for use in Performance assessment for Radioactive Waste Disposal", Reliability Engineering and System Safety 42, 1993.

[7] Jet Propulsion Laboratory, California Institude of Technology, http://www2.jpl.nasa.gov.tr/srtm/srtmBibliography.html visited on September 2006.

[8] Terma Space www.terma.com visited on June 2010.

[9] R. Zenick, T. J. McGuire, "Lightweight low-power coarse star tracker", 17th Annual AIAA/USU Conference on Small Satellites, 2003.

[10] O. Montenbruck, M. Garcia-Fernandez, J. Williams, "Performance comparison of semicodeless GPS receivers for LEO satellites", GPS Solut (2006) 10: 249 – 261.

[11] C. C. Liebe, "Accuracy performance of star trackers – A Tutorial", IEEE Transactions On Aerospace and Electronic Systems Vol. 38No. 2 April 2002 p. 587 – 589.

[12] C. C. Liebe "Star trackers for attitude determination", IEEE AES Systems Magazine, June 1995 p. 10 – 16.

[13] Hirvonen R. A., "On the statistical analysis of gravity anomalies. Publications of the institute of the International Association of Geodesy, Vol 37 1962, Helsinki.

[14] Hoffmann-Wellenhof B. and Moritz H., "Physical Geodesy", Second Edition, Springer Wien, 2006 New York.

Vitae - The author graduated from Middle East Technical University as Civil Engineer in 2003. He obtained his Master of Science degree from geodesy and photogrammetry division in 2006 in METU. In 2009 he obtained his PhD degree in METU from construction management division. The author works as Assistant Proffessor at Yüzüncü Yıl University at the department of Civil Engineering. Photogrammetry, GIS, Remote Sensing, Inertial Navigation Systems, Machine Control and Optimization are the study subjects of the author.